CHAPTER 3
Materials Collection and Characterization

3.1 Introduction

This chapter details the samples procurement sites along with various characterization techniques used for the understanding of the waste material. Geographical, physical, and historical data related to the sampling sites of the materials are covered to understand the environmental impact on the surroundings. X-Ray Diffraction (XRD), X-ray fluorescence (XRF), and scanning electron microscopy (SEM) characterization methods are also explained in detail to give the understanding of the techniques.

3.2 Fly Ash

The samples of Fly Ash were collected from its disposal site (29° 10' 31.371" N and 73° 59' 21.066" E) of Suratgarh Super Thermal Power Plant with the capacity of 1500 MW located near Suratgarh, district Sri Ganganagar, Rajasthan, India (Fig. 3.1). The power generation capacity of the plant is 1500MW. In the year 2016–2017, the power plant generated about 169.25 megatons of fly ash by burning 509.46 megatons of coal (CEA Report, 2015). From the data of 155 installed thermal power plants, there was 169.25 million tons of fly ash generated during the year 2016-17 from the burning of 509.46 million tons of coal.

There are two different types of samples, which were collected for the analysis to represent different age of fly ash:

(i) Fresh fly ash samples, which have been generated directly from the hopper (designated as FA-1)

(ii) Weathered fly ash samples collected from the dumping site after 30 days from its disposal (designated as FA-2)

These samples are collected in dry form into airtight containers.

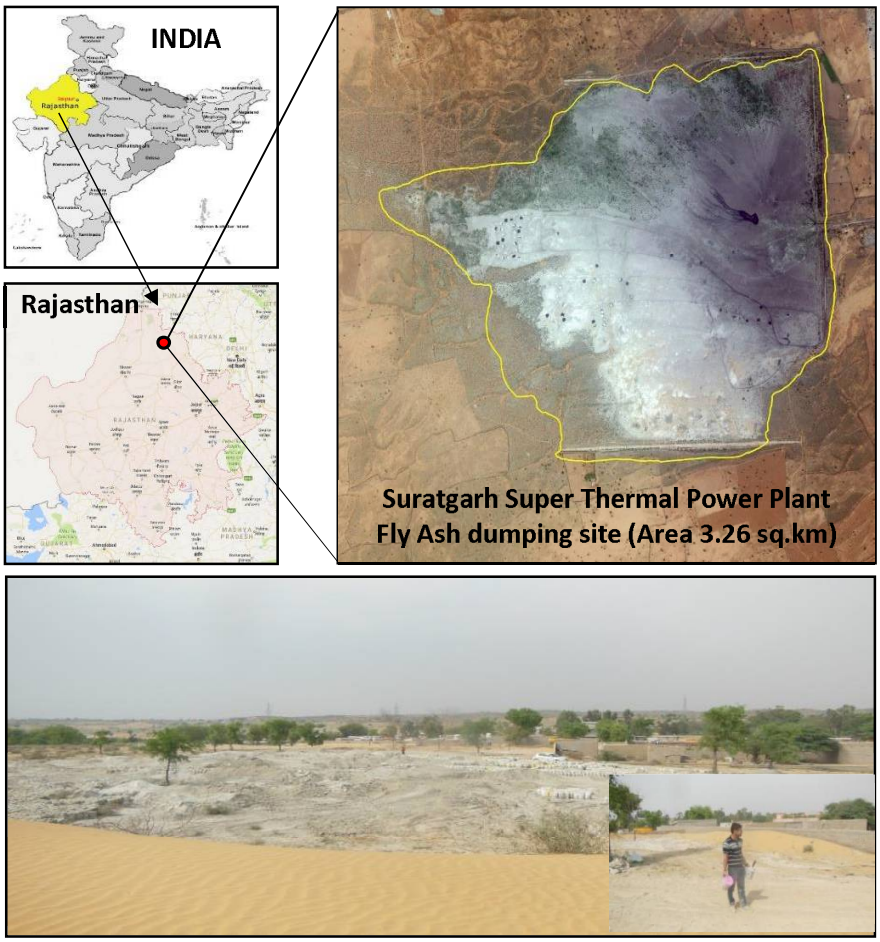

Fig. 3.1 Dumping fly ash site near Suratgarh Super thermal power plant, Suratgarh, Sri Ganganagar, Rajasthan, India

3.3 Copper Tailings

The copper tailings samples were taken from CT pond (Fig. 2) near Khetri Copper Complex, Hindustan Copper Limited (HCL) district Jhunjhunu, Rajasthan, India. The sampling site (27° 49' 59' N, 75° 46' 0" E) is in the hot semi-arid region of Aravalli fold of western India majorly having older alluvial soil (Ground Water Brochure, 2008). It accommodates an 80 km long metallogenetic region spreading from Singhana to Raghunathgarh, called Khetri Copper Belt of Jhunjhunu district.

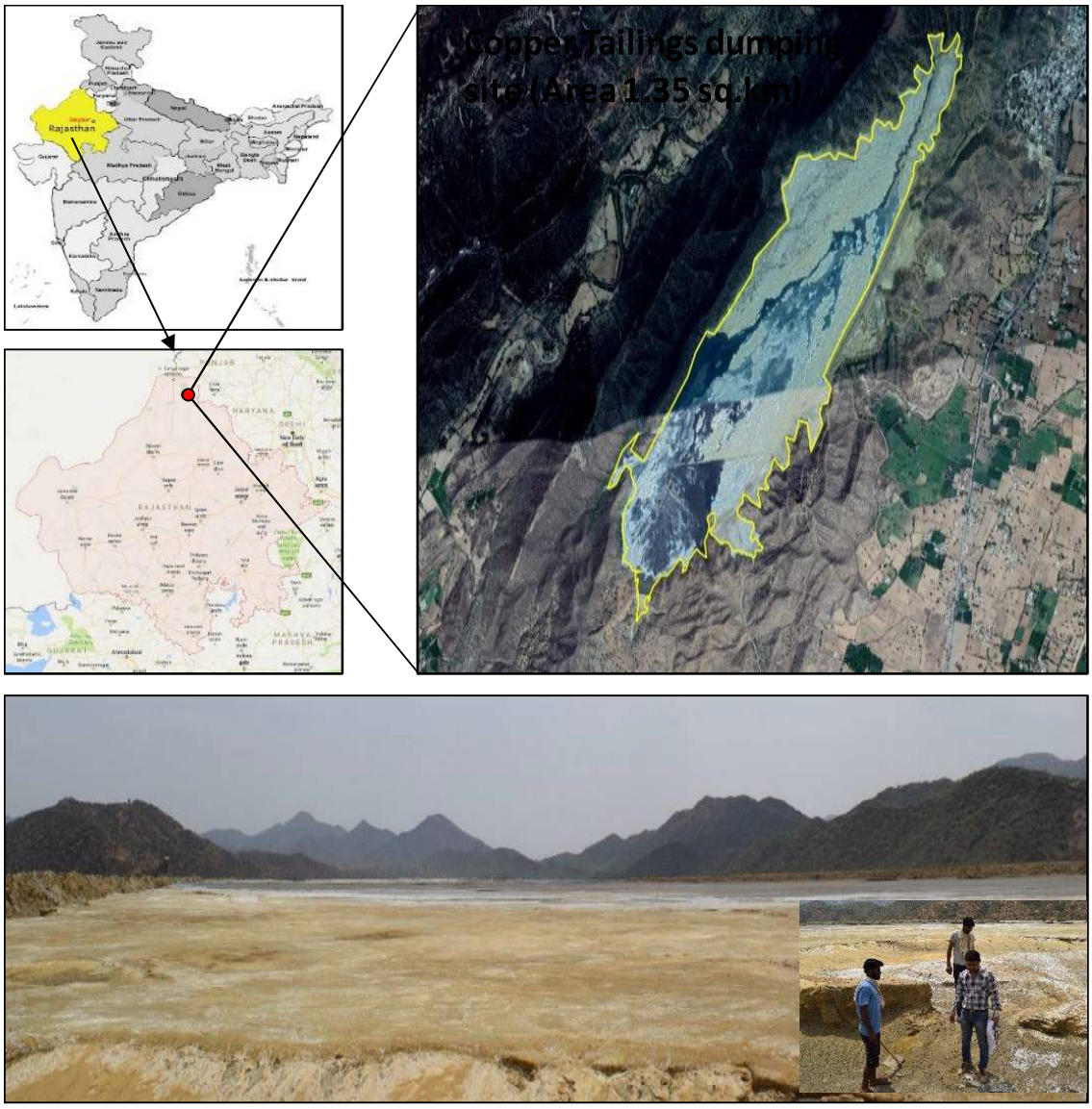

Fig. 3.2 Copper tailings dumping site near Khetri Copper Complex, Hindustan Copper Limited (HCL) district Jhunjhunu, Rajasthan, India

The ores in the region are enriched with Au, Ag, Co, Fe, U, and rare earth elements along with Cu (Sarkar and Gupta, 2012). The development process was initiated by the National Mineral Development Corporation (NMDC). It has been taken over by HCL after its formation in 1967.

3.4 Groundwater Samples

The actual scenario of the potential impact on groundwater near the disposal location of fly ash and tailings has been assessed by collecting and analyzing the groundwater sample from different locations. A total of ten groundwater samples are collected near Khetri copper tailing pond (Table 3.1), and seven groundwater samples (Table 3.2) are collected near fly ash dumping site of Suratgarh super thermal power plant.

Table 3.1 Location of sites for the sampling of groundwater near copper tailing pond

S.N.	Site Name	Sample number	Distance from disposal site (in km)	Position	Elevation (in m)
1	Gothra	S-1	2.91	28°03'55.75"N-75°49'27.39"E	379
2	Dhani Bhajnawali	S-2	2.45	28°03'02.94"N-75°49'16.96"E	358
3	Nanoowali	S-3	1.45	28°02'33.68"N-75°47'53.45"E	376
4	Rajota	S-4	2.87	28°01'48.72"N-75°41'09.17"E	370
5	Kharia Kua	S-5	4.77	28°00'50.95"N-75°47'06.27"E	390
6	Ward No. 19	S-6	4.88	28°00'47.07"N-75°47'15.71"E	396
7	Chirani	S-7	5.53	28°01'14.89"N-75°50'09.47"E	376
8	Khetari Town	S-8	6.32	27°59'58.08"N-75°47'10.04"E	407
9	Ward No. 13	S-9	6.58	27°59'48.96"N-75°47'14.93"E	415
10	Khetari Rural	S-10	6.75	27°59'44.05"N-75°47'11.66"E	428

Table 3.2 Location of sites for the sampling of groundwater near Suratgarh super thermal power plant

S.N.	Site Name	Sample number	Distance from disposal site (in km)	Position	Elevation (in m)
1	Somasar	S-1	3.7	29°12’20.50"N-74° 3'42.06"E	188
2	Somasar	S-2	3.8	29°11’47.5"N-74° 3’39.9"E	188.5
3	Rayanwali	S-3	4.4	9°10'58.88"N-73°56'46.57"E	188
4	Ladana	S-4	13.19	29°11'4.04"N-73°51'14.77"E	187
5	Ladana	S-5	13	29°11’4.3"N-73°50’15.69"E	187
6	Near SSTPP	S-6	1.97	29°10’28.03"N-74°00’42.89"E	187
7	Near SSTPP	S-7	2.1	29°10’57.22"N-74°00’55.57"E	199

3.5 X-Ray diffraction (XRD) Analysis and Results

The qualitative and quantitative analysis of the material is being served by the X-ray diffraction analysis for more than past one century. There are a lot of techniques associated with XRD analysis based on the scattering, emission and adsorption behavior of X-ray radiation. The chief and mostly used technique is the powder method in which the samples used for analysis were in powdered form.

This method is most commonly used to determine the structural property of the material. A diffraction pattern is exhibited by materials, which consists of a well-organized array and inherent atoms. This technique (also referred to as Debyr-Scherrer) is a nondestructive method of XRD analysis. The monochromatic X-rays are diffracted by the powdered sample. The basic principle behind the instrument used to perform XRD analysis is consist of three main parts viz. X-ray tube,

specimen holder, and detector. In the generation of X-ray process initially, a filament (usually made of copper) is heated in cathode ray tube to generate electrons. Then the high voltage is applied to accelerate the electron on the way to the sample, and finally, the target material is bombarded with these electrons. During the bombarding time, when the energy of the electron is enough to remove the electron from the inner cell of the sample, the X-Ray is started to generate. The anode might be made of copper, cobalt or molybdenum, but copper is most common and universally used material for this. The produced X-ray is filtered to form monochromatic X-rays having a single unique wavelength by using foils or different crystal monomers. The CuKα=1.5418 Å is generally considered for this operation.

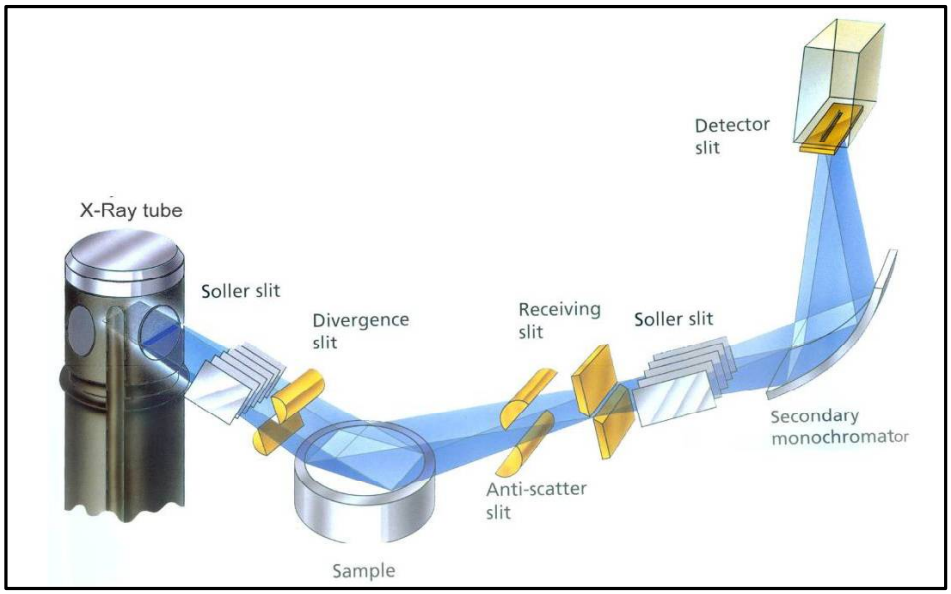

Fig. 3.3 Basic schematic representation behind powder X-Ray diffraction (PANalytical, 2013)

After the initial setup process, a finely grained material is put in a smallholding disc to distribute them evenly on the surface to form a thin flat layer. The essential fundamental law followed in this technique can be described using equation 3.1:

$$n\,\lambda = 2\,d\,\sin\theta \quad \text{----------} \quad \mathbf{3.1}$$

where,

λ = X-ray wavelength,

d = Spacing of atomic planes,

θ = Scattering angle,

n = Integer giving the order of the peal form in diffraction.

There is a formation of the cone when the powdered sample gives constructive interference after interaction with X-rays and follow Bragg's law. These cones have appeared in all the possible directions. To capture this, a circle like a film is available in the instrument. Every cone crosses the film exhibits diffraction line. The lines are the arcs and made up of several small patched, which formed from different individual crystals. These continuously distributed small patches used to appear as lines. The final diffracted X-rays are captured and counted after processing. The whole system is so arranged that there is a rotation of 2θ angle in the mounted arm (used to collect diffracted X-rays) when the sample rotates with angle θ in the way of collimated X-ray. Due to this successive rotation, a continuous observation of intensity of X-ray is essential.

Peak intensity is observed when the d- space in lattice planes available in the samples are fitted with the angle θ of the X-rays. Generally, the data captured by setting the angle between 5°-70° for the values of 2θ in the instrument. The partial in powdered samples are randomly oriented, and hence, this high range of angle is used to measure all possible diffraction pattern in a different direction.

As the d-space value is unique for all the mineral inherent in the samples, the diffraction peaks are converted to d-spacing to identify these minerals. It is done by following the available reference database. Following are the significant information about the tested samples reveals from the XRD analysis results:

A. the location of the maximum defection
B. different peak intensities
C. how the distribution of intensity varies with the diffraction angle.

The results are plotted in the form of a chart between 2θ and intensity, also referred to as diffractogram. The X-ray Diffraction (XRD) analysis for both fly ash and copper tailings has been done using RigakuMiniFlex II equipment with Cu-Kα (1.54 Å) radiation at Birla Institute of Technology and Science, Pilani.

3.5.1 Fly ash XRD analysis results

The results of mineralogy, done by XRD analysis, are shown in Fig. 3.4. It signifies that there are abundance of Bavenite ($Al_2Be_2Ca_4H_2O_{28}Si_9$), Silicon Oxide Quartz (SiO_2), Berlinite (AlO_4P), Magnesium chromate ($CrMgO_4$) minerals and minor occurrence of Rodalquilarite ($ClFe_2H_3O_{12}Te_4$), Milarite ($Al_{0.45}Be_{2.55}Ca_4H_{2.72}K_{1.184}Na_{0.24}O_{30.68}Si_{12}$) and Titanium (III) nitride Osbornite (NTi) and Strontium (Sr) minerals in the fly ash, which majorly contain Al, Be, Ca, Cr, Fe, Mg, Si, and Ti.

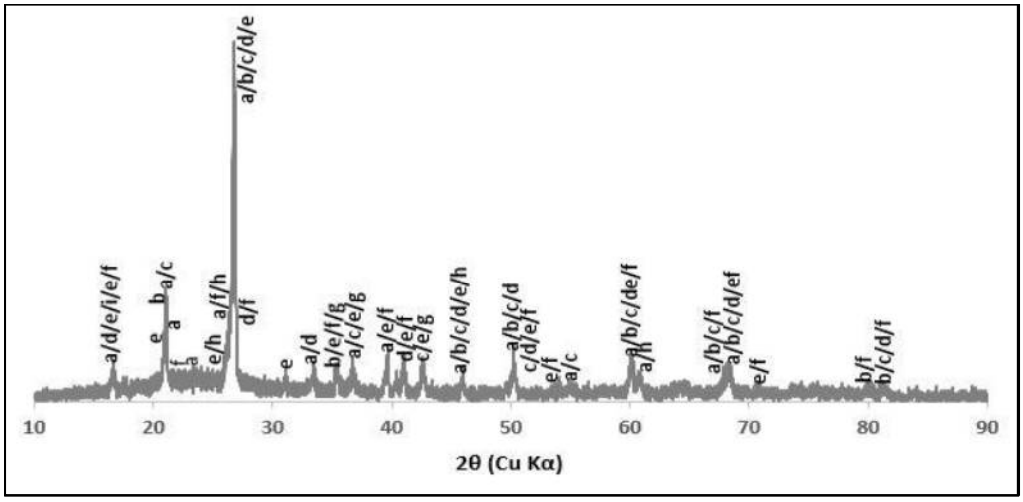

a: Bavenite ($Al_2Be_2Ca_4H_2O_{28}Si_9$)

b: Silicon Oxide Quartz (SiO_2)

c: Berlinite (AlO_4P)

d: Magnesium chromate - $-beta ($CrMgO_4$)

e: Rodalquilarite ($ClFe_2H_3O_{12}Te_4$)

f: Milarite ($Al_{0.45}Be_{2.55}Ca_4H_{2.72}K_{1.184}Na_{0.24}O_{30.68}Si_{12}$)

g: Titanium (III) nitride Osbornite (NTi)

h: Strontium (Sr)

Fig. 3.4 XRD results of fly ash

3.5.2 Copper tailings XRD analysis results

Inherent mineral available in copper tailings were Calcite ($CaCO_3$), Iron Sulphate ($Fe_2(SO_4)_3$), Chalcopyrite ($CuFeS_2$ -FeO (OH)), Yoderite ($Mg_2(Al, Fe^{3+})_6 Si_4O_{18}(OH)_2$), Zangoboite ($TiFeSi_2$), Iron Silicon (FeSi), Nickel Arsenide (Ni_5As_2), Iron Zinc ($FeZn_7$), Quartz (SiO_2), Jarosite ($K(Fe^{3+})_3(OH)_6(SO_4)_2$), Copper Tennantite ($Cu_{12}As_4S_{13}$), Copper Iron Arsenic

Sulfide $(Cu,Fe)_{12}As_4S_{13}$ (Sr). The major elements identified in copper tailings are Al, As, Ca, Cu, Fe, Ni, Ti, S, Si, Sr, and Zn.

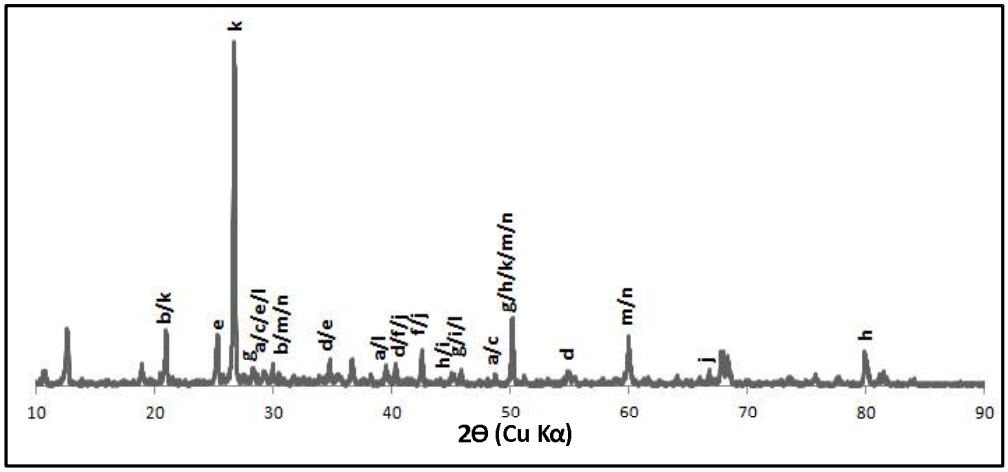

a: Calcite ($CaCO_3$)
b: Iron Sulphate ($Fe_2(SO_4)_3$)
c: Chalcopyrite ($CuFeS_2$)
d: Geothite (α-FeO (OH))
e: Yoderite ($Mg_2(Al, Fe^{3+})_6 Si_4O_{18}(OH)_2$)
f: Zangoboite ($TiFeSi_2$);
g: Iron Silicon (FeSi)
h: Iron Silicide (FeSi)
i: Nickel Arsenide (Ni_5As_2)
j: Iron Zinc ($FeZn_7$)
k: Quartz (SiO_2)
l: Jarosite ($K(Fe^{3+})_3(OH)_6(SO_4)_2$)
m: Copper Tennantite ($Cu_{12}As_4S_{13}$)
n: Copper Iron Arsenic Sulfide $(Cu,Fe)_{12}As_4S_{13}$ (Sr)

Fig. 3.5 XRD results of copper tailings

3.6 X-ray Fluorescence (XRF) Analysis and Results

The XRF analysis is performed to determine the elemental composition of the sample. The chemistry of the material is studied through the secondary X-Ray (fluorescent X-ray) emitted by the test material after it is exited from the primary source of X-ray. Every element has its unique characteristic X-ray and analyzing of those secondary X-ray makes this method very useful for the qualitative and quantitative analysis of sample material composition.

In this process, the material is exposed to high energy X-rays using an X-ray tube in a controlled manner. An inner shell electron of the atom in the sample is released out due to the application of bombarding X-rays having energy higher than the binding energy of the K or L shell. The stability of the atom regained as the electron of higher energy out shell of the atom fills the vacant position of the inner shell. In the movement of an electron from higher to lower energy fluorescent X-ray released. This released fluorescent X-ray has the same energy as the difference in the energy of two different quantum state of the electron. In XRF, the energy corresponds to this fluorescent X-ray is measured to identify the chemistry of the material. The chemical compositions of FA and CT have been found out by X-ray Fluorescence (XRF) using Panalytical Epsilon-5 available at Instrumentation Research Laboratory in Jawaharlal Nehru University, New Delhi. The samples in XRF analysis are prepared by initially pressing the material to make uniform powder, and then binder (boric acid) is added to form pellets using cylinder type dies. The analysis of these samples was done at 25 kV of voltage and 0.5 mA of current.

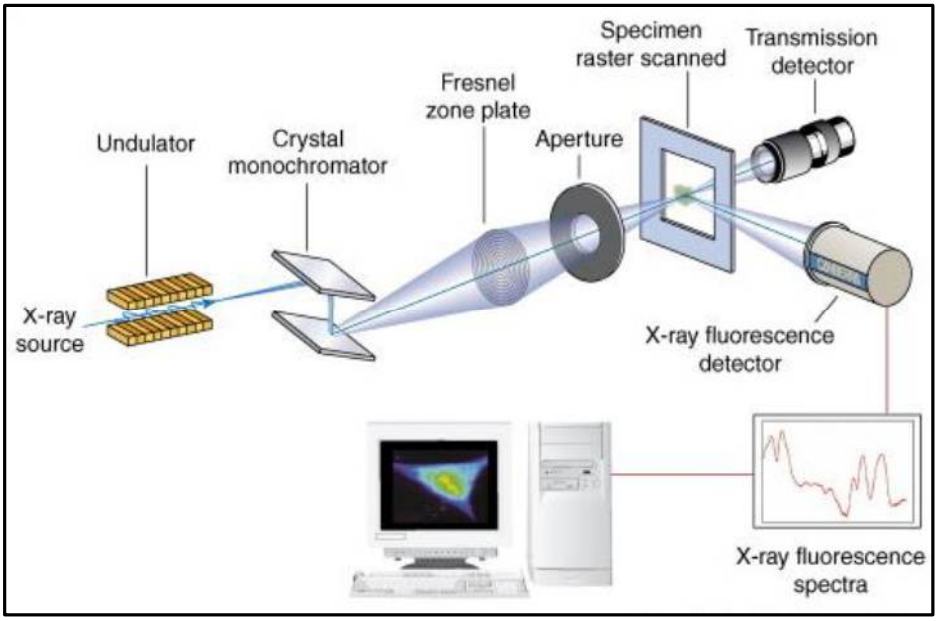

Fig. 3.6 Basic schematic representation behind X-Ray Fluorescence Spectroscopy (Fahrni, C.J., 2007)

3.6.1 XRF analysis results of fly ash, copper tailings and ordinary Portland cement (OPC)

XRF analysis results of fly ash, copper tailings, and OPC are presented in Table 3.3. The results reveal that the lime (CaO) content is very less in both CT and FA. However, SiO_2 has been found in a very high amount in both CT and FA. A significant amount of Al_2O_3, Fe_2O_3, and MgO is available in all the three tested materials.

Table 3.3 XRF analysis results of fly ash, copper tailings, and OPC

Chemical Constituents	OPC Grade 43	CT	FA
SiO_2 (%)	20.27	65.19	69.26
Al_2O_3 (%)	5.32	8.81	23.51
Fe_2O_3 (%)	3.56	12.93	3.33
CaO (%)	60.41	1.48	0.51
MgO (%)	2.46	3.98	0.62
SO_3 (%)	3.17	-	-
K_2O (%)	-	0.92	1.14
TiO_2 (%)	-	0.30	1.03

3.7 Scanning Electron Microscope (SEM) Analysis and Results

In SEM analysis, sample surface has been kept in a vacuum and an electron beam, focused by electromagnetic lenses, was applied on the surface.

A scanning electron microscope (SEM) is a type of electron microscope that produces images of a sample by scanning the surface with a focused beam of electrons. Initially, all the surface of the material is captured through the beam. The scattered electron from the surface of the sample was initially sent to the detector and then after amplification, it was sent to cathode-ray tube. In this tube, the information of the sample can be visualized in the form of an image. A typical SEM process diagram is shown in Fig. 3.7.

The instrument is made of a heated filament, electron beam source, lenses for the condensing, and cathode ray tube to form the image. In SEM, the magnified images are created with the help of electrons in place of light. The incident beam went from the lens and surrounded to the electromagnetic field. The lens focuses the beam to the sample, and as the beam hits the material, the X-rays and electrons are emitted by the sample. The mounted detectors capture the X-rays and electrons (backscattered and secondary). These collected X-rays and electrons are converted to signals by sensors and conveyed to a screen, which displays the magnified image on the sample. Carbon tape is used to hold the sample and kept on the sample holder. SEM can be used to study the surface morphology of different kind of samples like ceramics, composites, metals and biological material analysis.

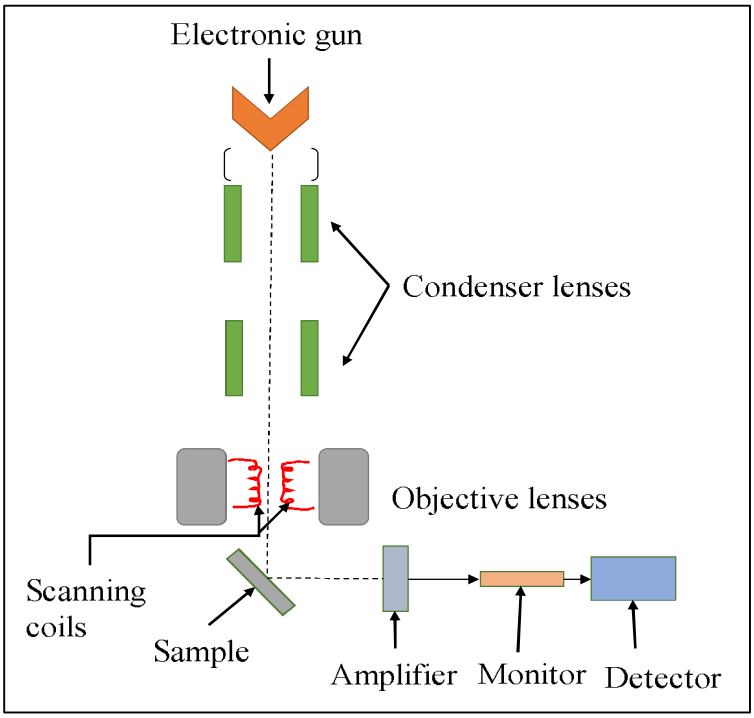

Fig. 3.7 Process followed in SEM analysis

In the current work, the SEM analysis of cement is studied by using the FEI Apreo-S instrument at Birla Institute of Technology and Science Pilani, Rajasthan, whereas, for FA and CT, it was done at Instrumentation Research Laboratory in Jawaharlal Nehru University, New Delhi using Zeiss EVO40.

3.7.1 SEM results of fly ash copper tailings and OPC

All the three materials are non-conductive; hence, before SEM analysis coating of silver was applied to the samples, and the instrument was operated at accelerating voltage of 15 kV and the working distance of 12.5 mm. The SEM images of FA, CT, and cement at different magnification are presented in Figs. 3.8, 3.9 and 3.10 respectively. The particles of FA are spherical, behaves like a ball bearing, which gave a greasy effect. CT particles are distributed unevenly with many irregularities in shape. The larger particles of CT have a smooth surface on which small particles are adsorbed.

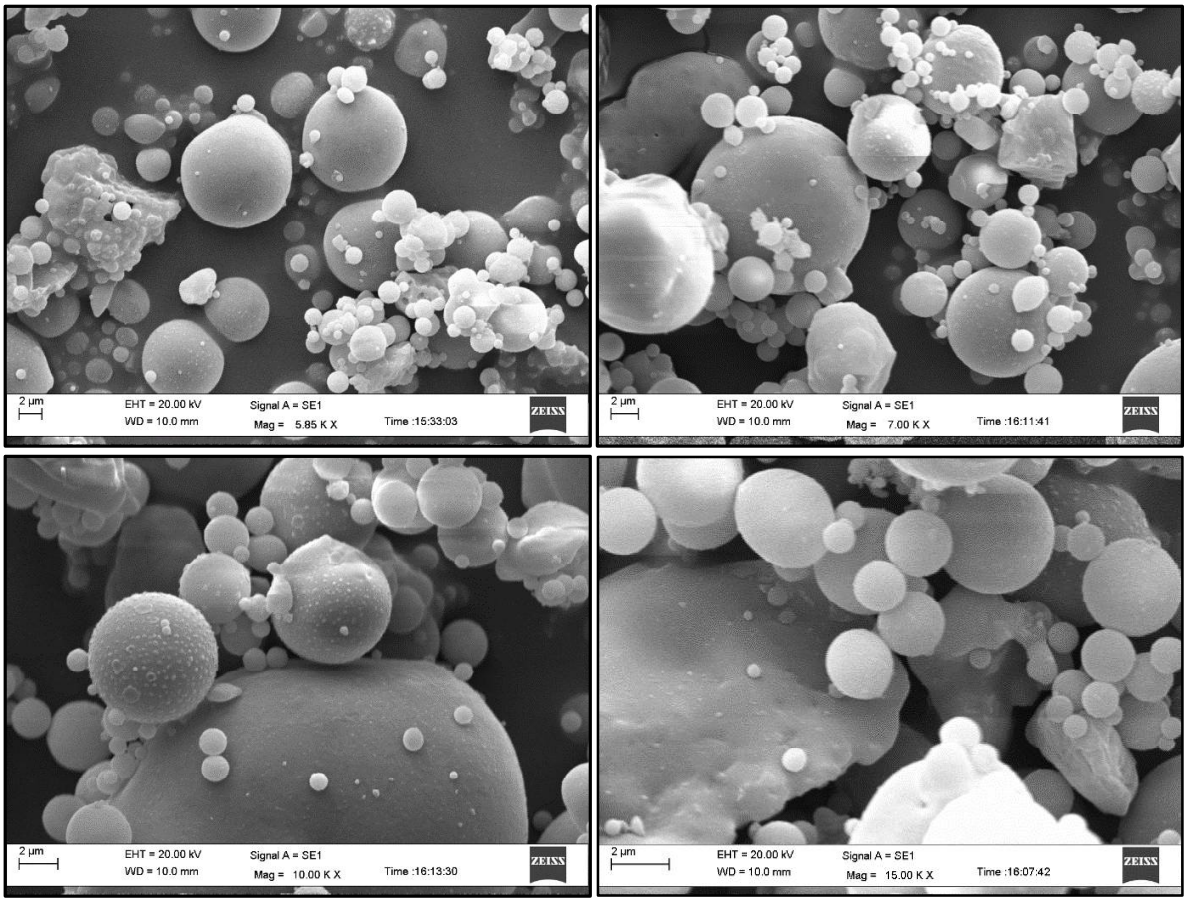

Fig. 3.8 Fly ash SEM results at different magnification levels

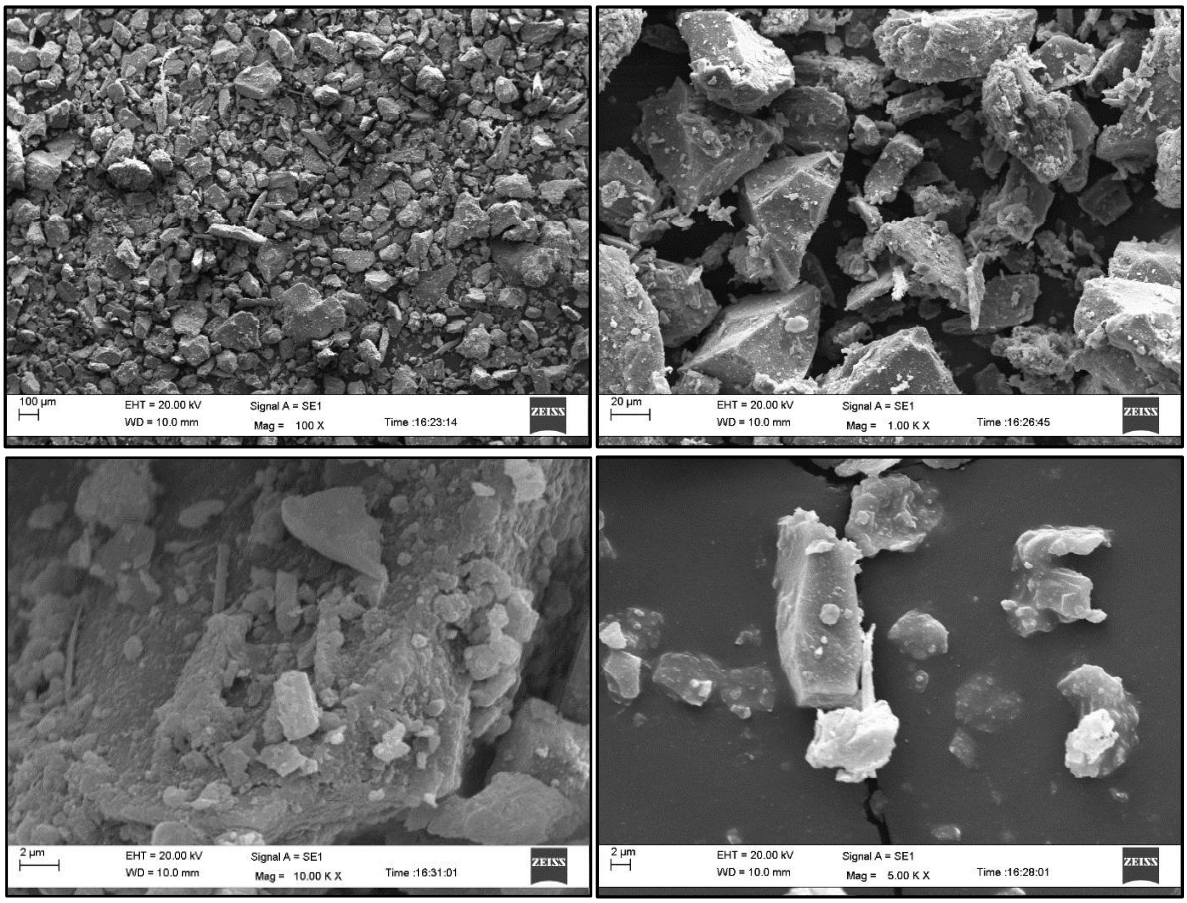

Fig. 3.9 Copper tailings SEM results at different magnification levels

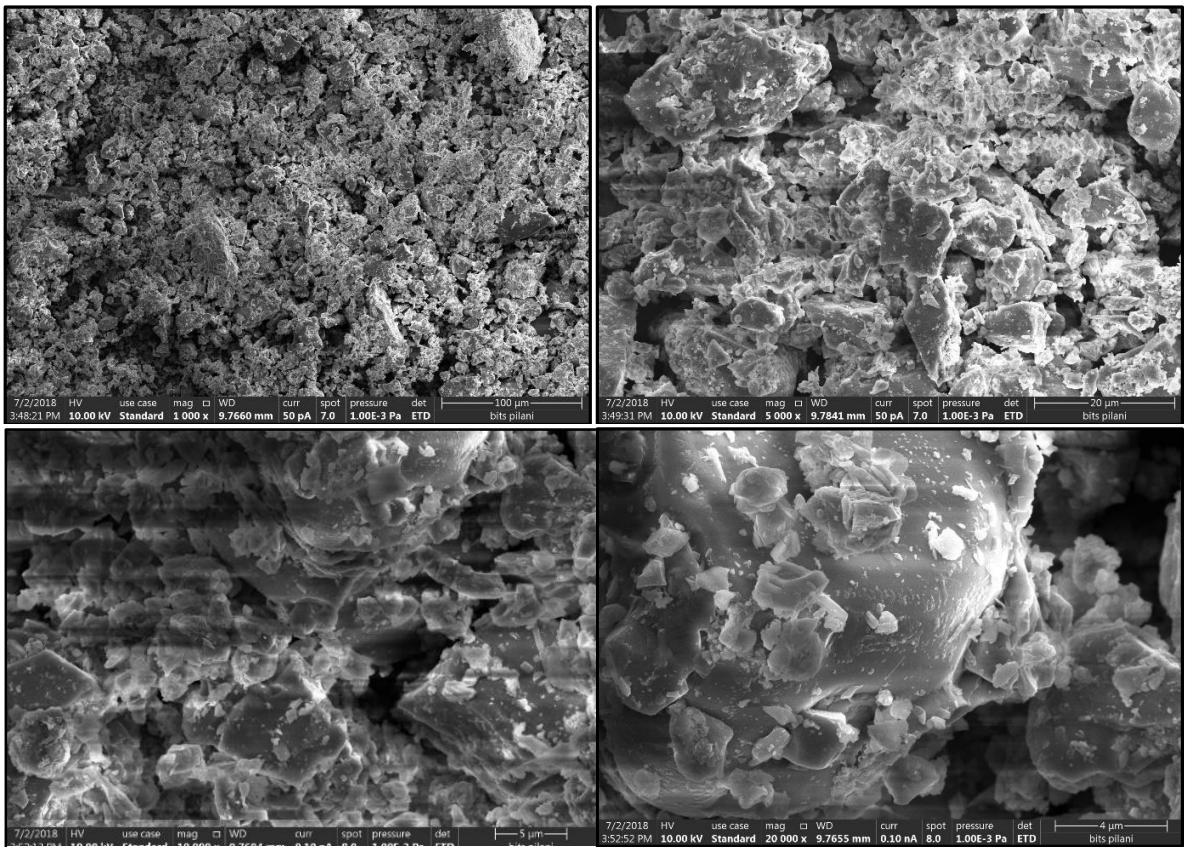

Fig. 3.10 OPC SEM results at different magnification levels

3.8 Physical Analysis

The physical properties of OPC, CT, and FA are presented in Table 3.3. Loss on ignition is measured according to IS 1727:2004. 1 g air-dried samples of the material have been taken in the crucible and put in the oven at 1000 ± 25°C for 20-30 min. In the oven, there must be provision for free air movement. After cooling, the samples were weighted and put for five more minutes in a muffle furnace. Again, the samples were weighted to determine the loss in weight after second heating to dry weight using equation 3.2.

$$\text{Loss on ignition (in percentage)} = \frac{A}{B} \times 100 \qquad \text{---------- 3.2}$$

where,

A = loss in weight,

B = weight of the sample (moisture free)

The moisture content of the cement, FA, and CT were measured by keeping sample material at 105 °C for 24 hours. After that, the difference in weight of the sample was calculated and divided by the dried sample as given in equation (3.3).

$$\text{Moisture content (in percentage)} = \frac{W_M - W_D}{W_D} \times 100 \quad \text{---------- 3.3}$$

where,

W_M = moist weight of the sample

W_D = dry weight of the sample

The density of OPC, fly ash, and copper tailings were calculated with regard to IS 4031 (part 11): 1995 as given in equation 3.4. The Le Chatelier flask was filled with kerosene (water-free) between 0 and 1mL mark. The remaining part above the liquid level was kept dry, and the flask was put in a water bath at room temperature. The initial reading was recorded. The material was poured & stopper was put on the flask. Then the flask was shaken horizontally to remove the air bubbles. The flask was kept in the water bath, and the final reading was noted. Then the specific gravity of material concerning water was calculated by dividing the calculated density with the density of water. Table 3.4 detailed the value of measured physical parameters in copper tailings, fly ash, and OPC.

$$\text{Density} = \frac{Mass\ of\ cement\ (in\ gram)}{Displaced\ volumn\ in\ cm^3} \quad \text{---------- 3.4}$$

Table 3.4 Physical parameters in copper tailings, fly ash and OPC

Physical parameter	**OPC Grade 43**	**CT**	**FA**
Loss on ignition (%)	1.87	2.00	2.3
Moisture (%)	0.20	0.15	0.30
Specific Gravity	3.15	3.20	2.10
Bulk density (kg/m^3)	1270	1420	940

The mass of the material per unit volume referred to as bulk density, which includes all the voids and air available inside the pores. Bulk density of all the materials is measured without the compaction.

3.9 Summary

An abundant amount of FA and CT is spread all over the sampling location in a haphazard manner. The dumping locations do not have any lining and separation from the surrounding. This improper handling of waste will lead to a possible adverse impact on the surroundings. The mineralogy and elemental analysis results, along with SEM images, gives a fair idea of the constituents and possible impact on the environment. In the next chapter of the thesis, leaching experiment results are presented to get more insights about the immobilization potential and its effect of groundwater.